# A Dynamic Nuclear Magnetic Resonance Study of Trimethylplatinum(IV) Halide Complexes of 1,1,2,2-Tetrakis(methylthio)ethane. Part 2.[1] High-temperature Fluxionality

**Edward W. Abel, Timothy P. J. Coston, Keith G. Orrell,* and Vladimir Šik**
*Department of Chemistry, The University, Exeter EX4 4QD*

The complexes $[PtXMe_3\{(MeS)_2CHCH(SMe)_2\}]$ (X = Cl, Br, or I) in $C_6D_5NO_2$ solution exist as *trans* and *cis*-1 isomers which, in the temperature range 333—423 K, exhibit novel fluxionality. This involves a *trans* ⇌ *cis*-1 interconversion which proceeds *via* a mechanism which exchanges *all* co-ordinated and unco-ordinated S–methyl environments and *all* Pt–methyl environments. The dynamics of this process were measured by $^1H$ n.m.r. band-shape analysis and two-dimensional exchange spectroscopy. Both methods yielded energy data in good agreement, $\Delta G^{\ddagger}$ (363 K) values being in the range 88.7—91.2 kJ mol$^{-1}$ for the three halogen complexes. Since $\Delta G^{\ddagger}$ values based on S–methyl and Pt–methyl exchanges were identical within experimental error a single concerted mechanism is operating. This is, in essence, a 1,3-metal-pivot process resulting from a rearrangement of individual Pt–S bonds and involving 109° clockwise or anticlockwise twists of the pendant $-CH(SMe)_2$ group about its adjacent C–C bond, bringing the other *gem* S-methyl into co-ordination with the metal. The fluxion proceeds *via* a highly non-rigid seven-co-ordinate platinum(IV) intermediate which effects exchange of all Pt–methyl environments. This is the first example of a metal-pivot process in mononuclear platinum(IV) complexes.

In an earlier paper[1] equimolar addition of the ligand 1,1,2,2-tetrakis(methylthio)ethane to trimethylplatinum(IV) halides was shown to produce mononuclear platinum(IV) complexes of type $[PtXMe_3\{(MeS)_2CHCH(SMe)_2\}]$ (X = Cl, Br, or I) as the predominant products. In deuteriochloroform solution these complexes exist predominantly as *trans* isomers with smaller amounts of *cis*-1 species (Figure 1). At solution temperatures between 213 and 333 K their $^1H$ n.m.r. spectra are sensitive to the pyramidal inversion rates of the two co-ordinated S atoms.[1] However, above *ca.* 373 K further gross changes occur, the cause of which will now be explored.

The ligand 1,1,2,2-tetrakis(methylthio)ethane contains four potential donor sites for co-ordination to a metal. Two of these sites have already been shown[1] to be involved in co-ordination to $Pt^{IV}$ at low temperatures. Since 1,3-metal shifts are well established in transition-metal complexes,[2] it is likely that co-ordination of all four S donors may occur at higher temperatures, which might account for the observed spectral changes. Such shifts have previously been restricted to dinuclear platinum(IV) complexes of types $[(PtClMe_3)_2(MeECH_2MeEMe)]$ (E = S or Se),[3] $[(PtXMe_3)_2(MeSCH_2SeMe)]$ (X = Cl, Br, or I),[4] $[(PtXMe_3)_2(SCH_2SCH_2SCH_2)]$ (X = Cl, Br, or I),[5] $[(PtXMe_3)_2\{HC(SMe)_3\}]$ (X = Cl or Br),[6] and chromium(0) or tungsten(0) pentacarbonyl complexes of types $[M(CO)_5(SCH_2SCH_2SCH_2)]$,[7] $[M(CO)_5(MeECH_2EMe)]$ (E = S or Se),[8] and $[M(CO)_5(MeSCH_2SeMe)]$.[9] The present ligand forms a chelate complex with $Cr(CO)_4$, namely $[Cr(CO)_4\{(MeS)_2CHCH(SMe)_2\}]$ but an attempt to identify any 1,3-metal ligand fluxionality failed on account of the limited thermal stability of this complex.[10]

We will now describe how $^1H$ n.m.r. spectral studies of $[PtXMe_3\{(MeS)_2CHCH(SMe)_2\}]$ (X = Cl, Br, or I) in the range 373—423 K afford the first example of 1,3-metal shifts in mononuclear platinum(IV) chelate complexes, and will propose a definitive mechanism for the process. The study also illustrates the power of two-dimensional exchange spectroscopy (EXSY) n.m.r. experiments for quantifying rates of complex high-energy fluxions.

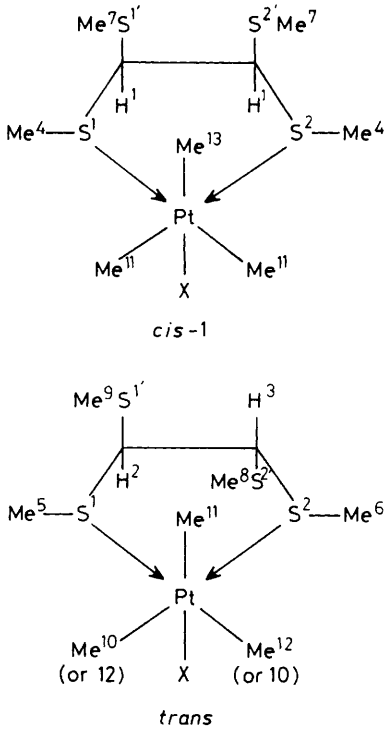


**Figure 1.** The *trans* and *cis*-1 configurational isomers of $[PtXMe_3\{(MeS)_2CHCH(SMe)_2\}]$ showing the hydrogen labelling

## Experimental

The complexes were prepared as described in the earlier paper.[1] Hydrogen-1 n.m.r. spectra were recorded on $C_6D_5NO_2$ solutions of the complexes, using a Bruker AM250 instrument operating at 250.13 MHz. The n.m.r. probe temperature was controlled as previously described.[1] Total band-shape analyses

were carried out using the authors' version of the DNMR3 program.[11] The $^1H$ two-dimensional EXSY experiments[12–15] on the S–methyl and Pt–methyl signals were performed using the same data table sizes as for the low-temperature experiments.[1] Optimum mixing times (*ca.* 1 s) were chosen to give greatest accuracy to the rate constants derived using the D2DNMR program.[15] Cross-relaxation effects of S–methyl and Pt–methyl hydrogens were assumed negligible as these signals exhibited no nuclear Overhauser enhancements.[16]

## Results and Discussion

Low-temperature n.m.r. studies of these complexes[1] showed that at 333 K pyramidal inversion of the two co-ordinated sulphur atoms, $S^1$ and $S^2$, was sufficiently rapid to average individual invertomers of the *trans* and *cis*-1 configurational isomers (Figure 1). At this temperature the *trans* signals have not fully sharpened due to the relatively high energy of the $S^1$ inversion. However, on warming to 373 K these signals become as sharp as all the other signals and so this temperature represents the fast-exchange limit for sulphur inversion in these complexes. All methine, S–methyl, and Pt–methyl proton signals may be confidently assigned at this temperature and the chemical shift and coupling constant data for all three complexes are collected in Tables 1—3. The $^1H$ n.m.r. spectrum of $[PtClMe_3\{(MeS)_2CHCH(SMe)_2\}]$ at 373 K is illustrated in Figure 2; the signal numbering refers to the labelled *trans* and *cis*-1 structures (Figure 1). In the methine region the *trans* isomer produces the distinctive AB quartet absorption; in the S–methyl region unco-ordinated SMe signals occur at lower frequencies than those of co-ordinated SMe signals with the latter exhibiting $^{195}Pt$ satellites [$^2J$(Pt–H) = 11—14 Hz]; in the Pt–methyl region axial methyls (*i.e. trans* to X) occur at lower frequencies than equatorial methyls (*i.e. trans* to S) and exhibit slightly larger $^2J$(Pt–H) couplings in the case of the Cl and Br complexes (Table 3). All three spectral regions show additional signals (labelled D) attributed to a small amount of the dinuclear complexes $[(PtXMe_3)_2\{(MeS)_2CHCH(SMe)_2\}]$ (X = Cl, Br, or I).[1] Isomer populations of the mononuclear complexes in $C_6D_5NO_2$ solvent (Table 4) can be seen to vary somewhat with halogen type.

On raising the solution temperature of the complexes from 373 to 423 K gross changes in band shapes occurred in all three spectral regions. In the methine region all signals broadened and the *trans* AB quartet began to coalesce with the *cis*-1 singlet. At the highest temperature reached this process was almost complete in the case of the iodo complex, but somewhat less so for the chloro and bromo complexes (Figure 3). These spectral changes, which are temperature reversible, are clearly the result

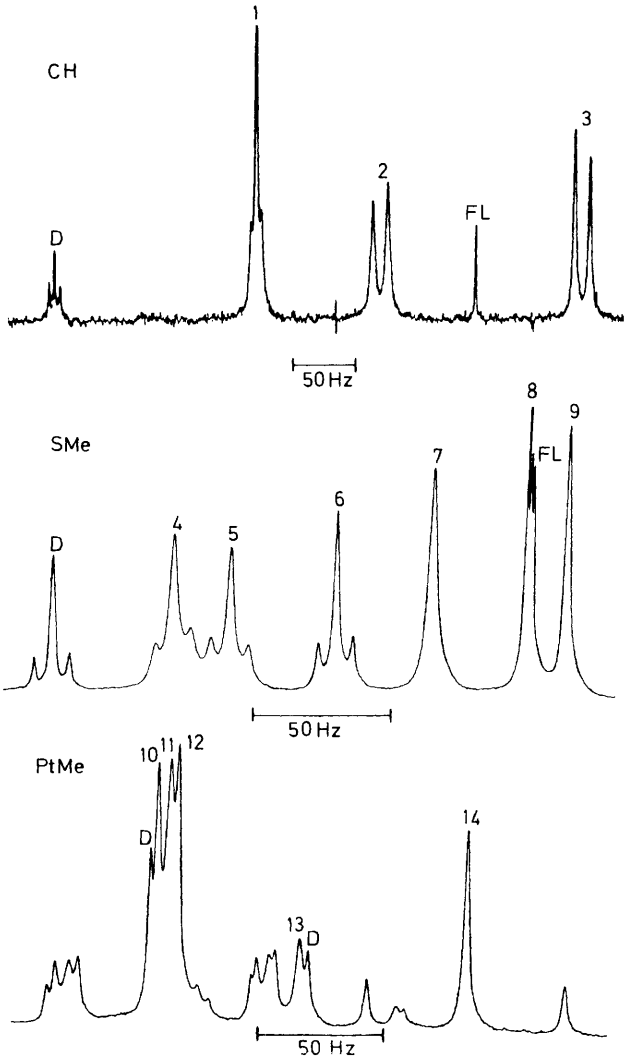


**Figure 2.** Hydrogen-1 n.m.r. spectrum of $[PtClMe_3\{(MeS)_2CHCH(SMe)_2\}]$ at 373 K showing the CH, SMe, and PtMe signals. Signal labelling refers to Figure 1. Unlabelled PtMe signals are $^{195}Pt$ satellites. D = Dinuclear complex impurity; FL = free ligand

**Table 1.** Hydrogen-1 n.m.r. parameters $[PtXMe_3\{(MeS)_2CHCH(SMe)_2\}]$ (X = Cl, Br, or I); methine region, 373 K

| | | δ | | | $^3J$(H–H)/Hz | | |
|---|---|---|---|---|---|---|---|
| Configuration | $^1H$ No. | Cl | Br | I | Cl | Br | I |
| *trans* | 2 | 4.46 | 4.57 | 4.77 | 11.65 | 11.64 | 11.71 |
| | 3 | 3.85 | 3.83 | 3.80 | 11.62 | 11.68 | 11.70 |
| *cis*-1 * | 1 | 4.85 | 4.89 | 4.90 | | | |

* $^3J$(Pt–H) = 7.8 (X = Cl), 8.24 (Br), and 8.52 (I) Hz.

**Table 2.** Hydrogen-1 n.m.r. parameters for $[PtXMe_3\{(MeS)_2CHCH(SMe)_2\}]$ (X = Cl, Br, or I); S–methyl region, 373 K

| | | | δ | | | $^3J$(Pt–H)/Hz | | |
|---|---|---|---|---|---|---|---|---|
| Configuration | | $^1H$ No. | Cl | Br | I | Cl | Br | I |
| *trans* | Co-ord. $S^1$ | 5 | 2.69 | 2.72 | 2.74 | 12.56 | 12.82 | 13.56 |
| | Co-ord. $S^2$ | 6 | 2.54 | 2.58 | 2.58 | 12.13 | 12.66 | 13.60 |
| | Unco-ord. $S^2$ | 8 | 2.28 | 2.29 | 2.28 | | | |
| | Unco-ord. $S^1$ | 9 | 2.22 | 2.24 | 2.25 | | | |
| *cis*-1 | Co-ord. | 4 | 2.77 | 2.84 | 2.92 | 11.61 | 10.88 | 11.72 |
| | Unco-ord. | 7 | 2.41 | 2.42 | 2.41 | | | |

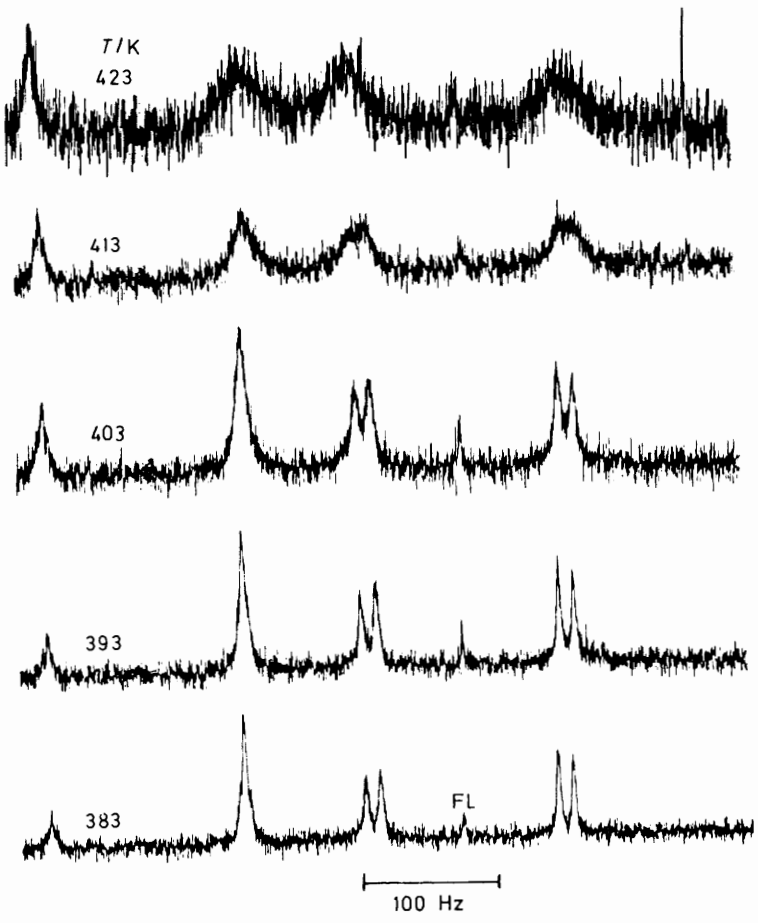


**Figure 3.** Variable-temperature $^1$H n.m.r. spectra of the methine signals of $[PtClMe_3\{(MeS)_2CHCH(SMe)_2\}]$; FL = free ligand

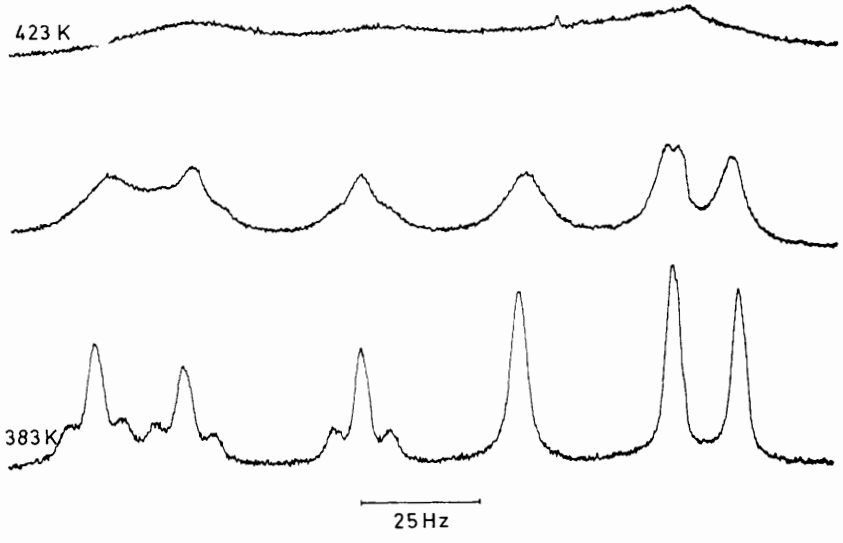


**Figure 4.** Variable-temperature $^1$H n.m.r. spectra of the S-methyl signals of $[PtClMe_3\{(MeS)_2CHCH(SMe)_2\}]$

of interconversion of *cis*-1 and *trans* isomers. In the S–methyl region initial increase in temperature causes the signals of *trans* and *cis*-1 co-ordinated SMe to coalesce and similarly those of the *trans* and *cis*-1 unco-ordinated SMe, followed ultimately by coalescence of all SMe signals (Figure 4). Thus a process is occurring which interconverts *trans* and *cis*-1 isomers *and* exchanges all co-ordinated and unco-ordinated SMe signals. Similarly gross broadenings occur in the Pt–methyl region.

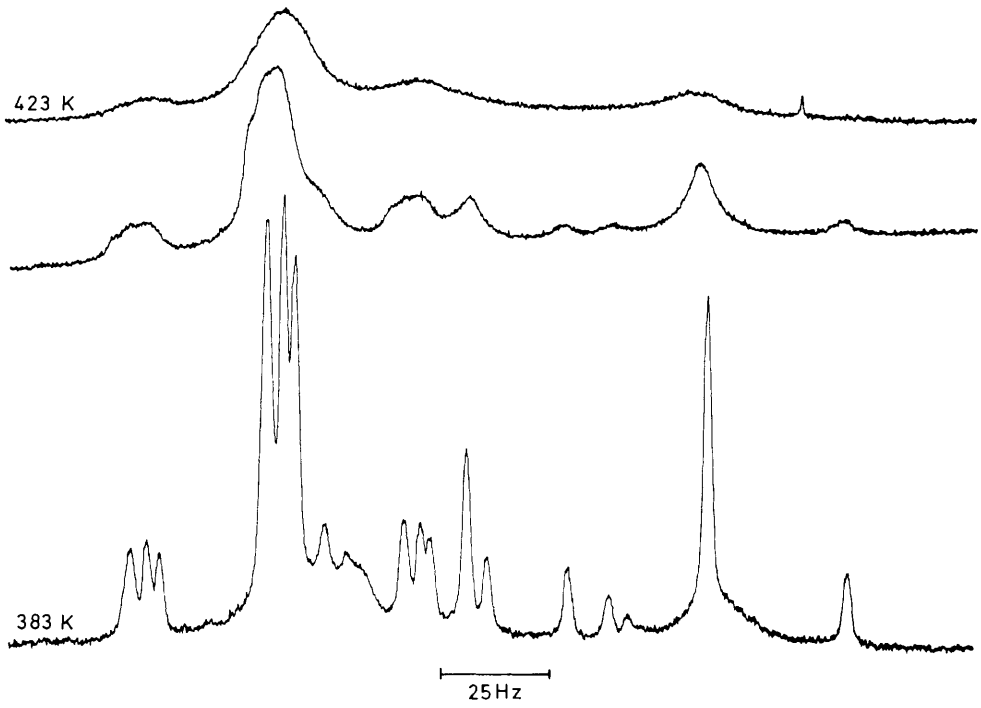


**Figure 5.** Variable-temperature $^1H$ n.m.r. spectra of the Pt–methyl signals of $[PtClMe_3\{(MeS)_2CHCH(SMe)_2\}]$

**Table 3.** Hydrogen-1 n.m.r. parameters for $[PtXMe_3\{(MeS)_2CHCH(SMe)_2\}]$ (X = Cl, Br, or I); Pt–methyl region, 373 K

| Configuration | PtMe *trans* to | $^1H$ No. | δ Cl | δ Br | δ I | $^2J$(Pt–H)/Hz Cl | $^2J$(Pt–H)/Hz Br | $^2J$(Pt–H)/Hz I |
|---|---|---|---|---|---|---|---|---|
| *trans* | X | 14 | 0.92 | 1.04 | 1.17 | 72.21 | 71.60 | 69.53 |
| | S | 10 | 1.38 | 1.47 | 1.61 | 71.15 | 71.39 | 71.20 |
| | S | 12 | 1.35 | 1.44 | 1.59 | 70.43 | 70.68 | 71.77 |
| *cis*-1 | X | 13 | 1.17 | 1.27 | 1.40 | 73.94 | 73.59 | 70.87 |
| | S | 11 | 1.36 | 1.46 | 1.61 | 71.25 | 71.30 | 71.77 |

**Table 4.** Configurational isomer populations for the complexes $[PtXMe_3\{(MeS)_2CHCH(SMe)_2\}]$ (X = Cl, Br, or I) at 373 K

| X | % Configuration *trans* | % Configuration *cis*-1 |
|---|---|---|
| Cl | 63.2 | 36.8 |
| Br | 66.9 | 33.1 |
| I | 75.3 | 24.7 |

Initially this involves exchange between equatorial *cis*-1 and *trans* PtMe sites and between axial *cis*-1 and *trans* PtMe sites, but is followed by exchange between all PtMe sites (Figure 5).

A rationalisation of these spectral changes was achieved by a combination of one-dimensional band-shape analysis and two-dimensional EXSY $^1H$ n.m.r. experiments.

*Total Band-shape Analysis.*—The only spectral region amenable to this treatment was the methine region. Even this was not ideally suited since full coalescence was not achieved at the highest attainable temperature (423 K) and the spectra had low signal-to-noise ratios due to the limited solubilities of the complexes in $C_6D_5NO_2$. Nevertheless, the analysis did provide insight into the mechanism of the ligand fluxion.

Previous studies[17,18] have described how sulphur chelate ligands undergo 180° rotations ('pancake flips') with respect to $PtXMe_3$ moieties. However, such a mechanism operating here would *not* exchange *trans* and *cis*-1 isomers nor would it lead to exchange of co-ordinated and unco-ordinated S–methyls. A mechanism which could achieve these effects would involve rearrangement of individual Pt–S bonds such that the previously unco-ordinated *gem* S–methyl is brought into co-ordination. By a sequence of two Pt–$S^1/S^{1'}$ and Pt–$S^2/S^{2'}$ rearrangements the isomers may be interconverted according to the scheme shown in Figure 6. Such a mechanism necessarily involves the *cis*-2 isomer and the other member of the *trans* (DL) pair (labelled *trans**). Even though there is no n.m.r. distinction between this *trans* pair both structures must be included in the dynamic spin problem (below). The methine protons are

$$\begin{array}{ccc} CC & \rightleftharpoons & AB \\ \Updownarrow & & \Updownarrow \\ BA & \rightleftharpoons & DD \end{array}$$

labelled here according to Figure 6. However, no *cis*-2 isomer was detected in $CDCl_3$ or $C_6D_5NO_2$ solution and thus the spin problem reduces to one with three configurations. When $^{195}Pt$ satellite signals are included, the dynamic problem becomes as shown below. The methine $^1H$ spectra should therefore be

$$\begin{array}{ccccc} CC \overset{k}{\rightleftharpoons} AB & & & CCX \overset{k}{\rightleftharpoons} ABX & \\ \quad k \quad k' & & & \quad k \quad k' & \\ BA & + & & BAX & \\ & & & X = {}^{195}Pt & \\ 66.6\% & & & 33.4\% & \end{array}$$

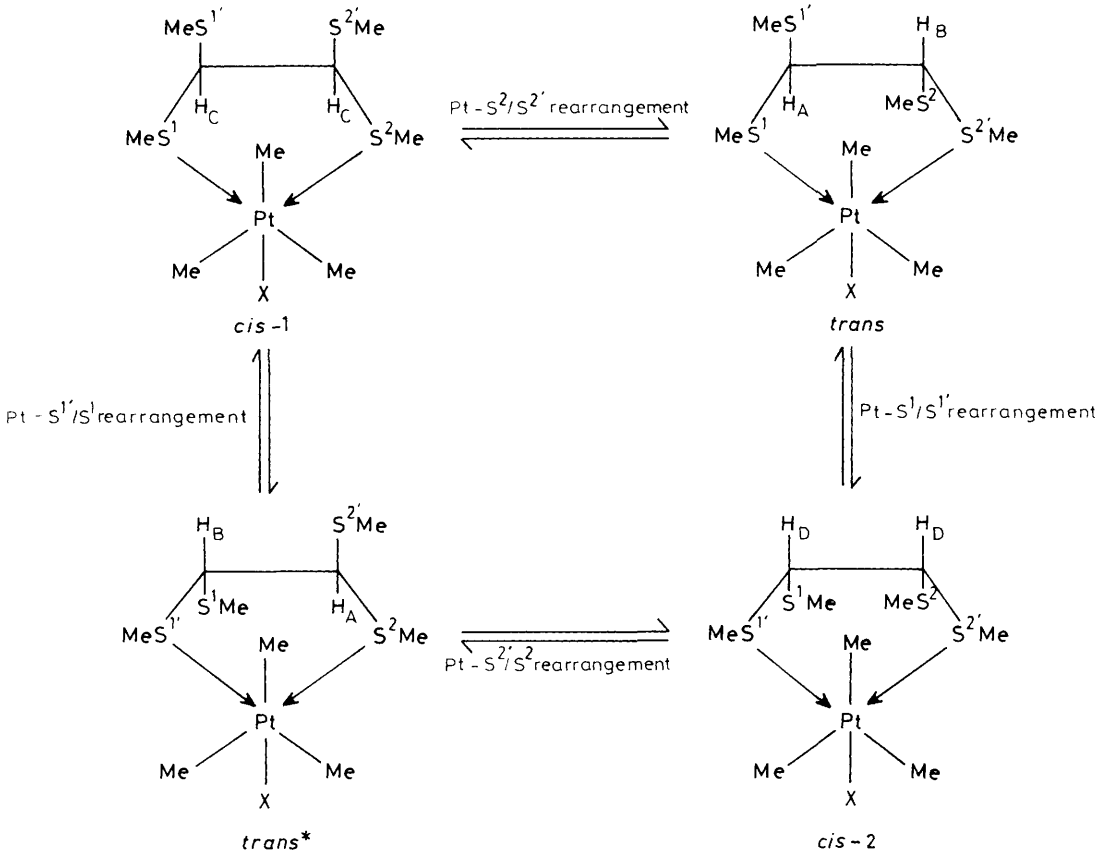


**Figure 6.** *cis–trans* Isomer exchange of $[PtXMe_3\{(MeS)_2CHCH(SMe)_2\}]$ complexes due to the 1,3-metal ligand fluxion arising from the Pt–S bond rearrangements

**Table 5.** Activation parameters for the *cis*-1/*trans* interconversion in the complexes $[PtXMe_3\{(MeS)_2CHCH(SMe)_2\}]$ (X = Cl, Br, or I)

| X | $E_a$/kJ mol$^{-1}$ | $\log_{10}(A/s^{-1})$ | $\Delta H^{\ddagger}$/kJ mol$^{-1}$ | $\Delta S^{\ddagger}$/J K$^{-1}$ mol$^{-1}$ | $\Delta G^{\ddagger}$/kJ mol$^{-1}$ |
|---|---|---|---|---|---|
| Cl | 93.4 ± 2.8 | 13.2 ± 0.4 | 90.0 ± 2.8 | −3.3 ± 6.8 | 91.0 ± 0.7 |
| Br | 95.0 ± 1.9 | 13.4 ± 0.3 | 91.6 ± 1.9 | 1.0 ± 4.8 | 91.3 ± 0.5 |
| I | 103.2 ± 2.4 | 14.9 ± 0.3 | 99.8 ± 2.4 | 30.7 ± 6.0 | 90.6 ± 0.6 |

sensitive to two rate constants $k$ (*cis*-1 ⟶ *trans*) and $k'$ (*trans* ⟶ *trans**). Theoretical spectra were simulated by varying $k$ and $k'$ independently, but satisfactory fittings with experimental spectra were achieved only when $k'$ was kept at zero, implying a negligible rate of direct *trans* ⇌ *trans** interconversions. This has important mechanistic implications which will be discussed later. 'Best fit' values of the rate constant $k$ in the temperature range 383—423 K gave activation parameters for the *cis*-1 ⟶ *trans* interconversion of reasonable precision (Table 5).

*Quantitative Two-dimensional Spectroscopy.*—The high temperature fluxionality of these complexes is clearly somewhat too slow to be well suited to one-dimensional band-shape analysis, and more reliable quantitative data are likely to be derived from two-dimensional experiments,[12–15] which are sensitive to appreciably slower exchange rates. Such experiments were therefore performed on the S–methyl and Pt–methyl regions of the spectra. The complexities of these regions in any case precluded any accurate band-shape analyses from being performed, but presented no difficulties for the two-dimensional approach.

*Sulphur–methyl region.* At 373 K this region consisted of six signals, three due to co-ordinated S–methyls and three due to unco-ordinated S–methyls (Figure 2). Two-dimensional EXSY spectra of the complexes in the temperature range 353—373 K revealed cross-peaks arising from exchange between all signals. This confirms the $^1H$ one-dimensional observations that *cis*-1 ⇌ *trans* interconversion exchanges *all* S–methyl environments. Of the spectra recorded in the range 353—373 K, those at 363 K provided the most favourable balance between diagonal and off-diagonal signal intensities and so this temperature was used for computing the rate constants. The spectrum of $[PtClMe_3\{(MeS)_2CHCH(SMe)_2\}]$ at 363 K is shown in Figure 7. Since all signals are undergoing exchange there are 30 cross-peaks in the exchange matrix. However, the full 6 × 6 matrix can be simplified for calculation of the single magnitude of rate constant involved. If the matrix be divided into four quadrants (Figure 7) the top-left and bottom-right quadrants contain only cross-peaks. Ideally, these should have identical total intensities. In practice, they differed slightly but were scaled to the same value as required by the D2DNMR program[15] and labelled 'CP.' The bottom-left-hand quadrant contains diagonal signals due to co-ordinated S–methyls and cross-peaks between signals due to co-ordinated *trans* and *cis*-1 SMe. Since the exchange of interest is that which interconverts signals of co-ordinated and unco-ordinated SMe, the contents of this quadrant may be summed and treated as a single signal, labelled 'D1.' The same treatment may be applied to the fourth quadrant 'D2' which contains signals due to unco-ordinated SMe and their mutual exchange cross-peaks. Thus, the problem

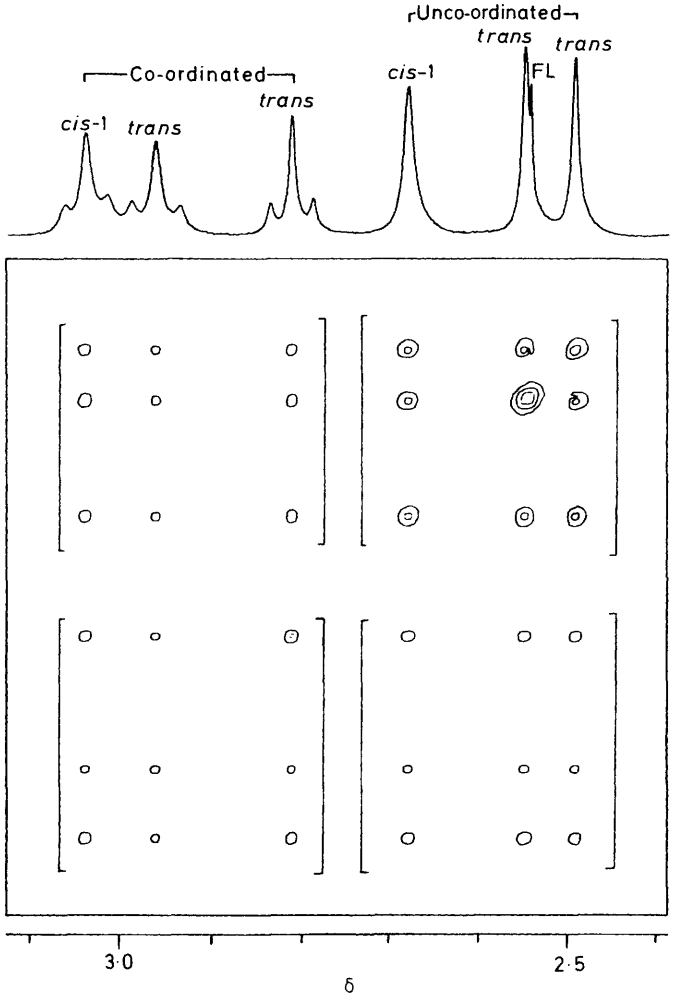


**Figure 7.** Hydrogen-1 two-dimensional EXSY spectrum of the S–methyl signals of $[PtClMe_3\{(MeS)_2CHCH(SMe)_2\}]$ at 363 K, showing how the total plot was divided into four quadrants

is reduced to a 2 × 2 exchange matrix. As corresponding *cis*-1 and *trans* isomer signals are always combined, the populations of the two composite signals 'D1' and 'D2' are now equal. Thus, the matrices required as input for the D2DNMR program are as shown below where the $I$ matrix is obtained by 90° clockwise

$$I = \begin{bmatrix} D1 & CP \\ CP & D2 \end{bmatrix} \qquad P = \begin{bmatrix} 0.5 \\ 0.5 \end{bmatrix}$$

rotation of the experimental two-dimensional EXSY plot. Matrix $J$ is then obtained from $I \cdot P^{-1}$, from which the kinetic matrix $L$ can be calculated. The off-diagonal elements of $L$ represent the required rate constant, $k$. This parameter was computed for all three complexes and activation energies, $\Delta G^{\ddagger}$ (373 K), calculated. The values are presented in Table 6 and compared with the values derived from the one-dimensional bandshape analyses of the methine region.

*Platinum-methyl region.* The *cis*-1/*trans* exchange process necessarily leads to a loss of distinction between the equatorial Pt–methyl environments, but no axial–equatorial exchange will arise providing the fluxionality is restricted to the ligand, L, moiety. Therefore, the observation of axial–equatorial Pt–methyl exchange indicates either additional fluxionality directly consequential to the ligand fluxionality or a totally independent fluxion. In order to explore these two possibilities, hydrogen-1

**Table 6.** Activation energies, $\Delta G^{\ddagger}$ (363 K),[a] for high-temperature fluxions in $[PtXMe_3\{(MeS)_2CHCH(SMe)_2\}]$

| | $\Delta G^{\ddagger}$ (363 K)/kJ mol$^{-1}$ | | |
|---|---|---|---|
| | *cis*-1 ⇌ *trans* | | |
| X | *b* | *c* | Pt–Me exchange |
| Cl | 91.2 | 90.6 | 90.6 |
| Br | 91.2 | 91.2 | 90.1 |
| I | 88.7 | 90.6 | 89.9 |

[a] All uncertainties ±0.5 kJ mol$^{-1}$. [b] Based on one-dimensional data (Table 5) adjusted to 363 K. [c] Two-dimensional.

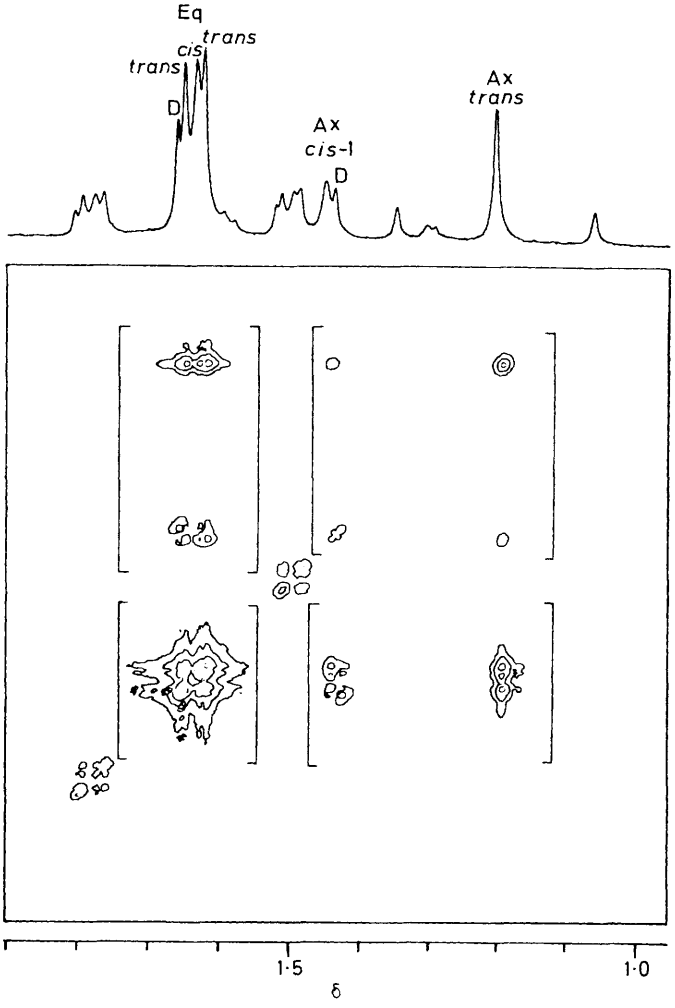


**Figure 8.** Hydrogen-1 two-dimensional EXSY spectrum of the Pt–methyl signals of $[PtClMe_3\{(MeS)_2CHCH(SMe)_2\}]$ at 363 K, showing how the signals were grouped into four sets

two-dimensional EXSY experiments were performed on the Pt–methyl regions of the $^1H$ spectra of all three complexes. The spectrum of $[PtClMe_3\{(MeS)_2CHCH(SMe)_2\}]$ at 363 K (Figure 8) may be taken as typical. It consists of two axial signals and three equatorial signals, all of which possess $^{195}Pt$ satellites. The two-dimensional EXSY spectrum contains cross-peaks between all the main signals indicating exchange between all Pt–methyl environments. The only exchange of particular interest is that between axial and equatorial environments, since

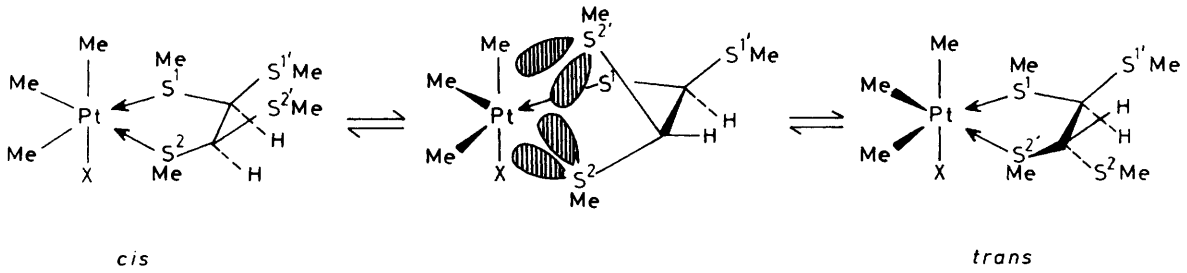


**Figure 9.** The mechanism of the 1,3-metal pivot process in the complexes $[PtXMe_3\{(MeS)_2CHCH(SMe)_2\}]$ which leads to *cis*/*trans* interconversion *via* a seven-co-ordinate platinum(IV) intermediate

**Table 7.** Energy data for ligand pivoting and related fluxions in trimethylplatinum(IV) bromide complexes

| Complex | Process | $\Delta G^{\ddagger}$ (298.15 K)/ kJ mol$^{-1}$ | Ref. |
|---|---|---|---|
| $[(PtBrMe_3)_2\overline{SCH_2SCH_2SCH_2}]$ | 60° Pt–S 1,3-pivot | 58.8 | 5 |
| $[(PtBrMe_3)_2\overline{SCH_2SCH_2SCH_2SCH_2}]$ | 90° Pt–S 1,5-pivot | 64.0 | * |
| $[(PtBrMe_3)_2\{HC(SMe)_3\}]$ | 60° Pt–S 1,3-pivot | 69.5 | 6 |
| $[PtBrMe_3(MeSCH_2SCH_2SMe)]$ | 180° Pt–S 1,5-switch | 78.0 | 18 |
| $[PtBrMe_3\{(MeS)_2CHCH(SMe)_2\}]$ | 109.5° C–C 1,3-pivot | 91.2 | This work |

* E. W. Abel, G. D. King, K. G. Orrell, V. Šik, T. S. Cameron, and K. Jochem, *J. Chem. Soc., Dalton Trans.*, 1984, 2047.

axial–axial and equatorial–equatorial exchanges resulting from the *cis*-1/*trans* isomer exchange have already been studied. Thus, in the two-dimensional EXSY spectral plots, *cis*-1 and *trans* equatorial signals and *cis*-1 and *trans* axial signals (diagonals plus mutual cross-peaks) are grouped together (Figure 8), and labelled 'D1' and 'D2' respectively. The other cross-peaks due to axial–equatorial exchanges are similarly combined into two sets and labelled 'CP'. Thus, the dynamic process is again reduced to a two-site problem, and the matrices used as input for the D2DNMR problem are of the form shown below where the population matrix, $P$, takes account of the 2/1

$$I = \begin{bmatrix} D1' & CP' \\ CP' & D2' \end{bmatrix} \quad P = \begin{bmatrix} 0.67 \\ 0.33 \end{bmatrix}$$

population ratio of equatorial/axial Pt–methyls. It should be noted that as it was not possible to detect and resolve all $^{195}Pt$ satellite signals these were omitted from the intensity matrices. The weak signals (D) due to the dinuclear complex could not be separated from the other signals in the intensity matrices and thus could be a possible minor source of error in the rate constant calculations. This procedure provided rate constants at 363 K for axial–equatorial Pt–methyl exchanges in all three complexes. Using the Eyring equation, $\Delta G^{\ddagger}$ (363 K) values were then calculated (Table 6). These values can be seen to be of the same magnitude as the values derived from the *cis*-1/*trans* isomer exchange, suggesting that the 1,3-metal pivot process and the Pt–methyl exchange processes are concerted and involve a common transition state.

Such a conclusion is compatible with previous findings. For example, in the chelate complexes $[PtXMe_3(MeSCH_2SCH_2SMe)]$ (X = Cl, Br, or I)[18] the ligand 180° rotations and Pt–methyl scramblings could be investigated independently and found to be concerted processes. Also, in the dinuclear platinum(IV) complexes, $[PtXMe_3)_2L]$, ligand switching occurs when L is $MeSCH_2SeMe$[4] and ligand 1,3-pivoting occurs when L is $HC(SMe)_3$.[6] In both these cases, the ligand movements involve concerted Pt–methyl scramblings. These processes involve highly non-rigid seven- or eight-co-ordinate platinum(IV) intermediates which cause averaging of all Pt–methyl environments. A similar situation must exist with the present $[PtXMe_3\{(MeS)_2CHCH(SMe)_2\}]$ complexes with the transition-state intermediate here being a seven-co-ordinate platinum(IV) species.

1,3-Metal pivoting processes have hitherto been observed only in dinuclear platinum(IV) complexes, and so this is the first observation of such a process in a mononuclear platinum(IV) chelate complex. The proposed mechanism involves rearrangements of individual Pt–S bonds caused by 109.5° (tetrahedral angle) pivots of the pendant $-CH(SMe)_2$ group about its attached C–C bond. Such a process brings the previously uncoordinated *gem* S–methyl into co-ordination with the platinum centre (Figure 9). By a sequence of Pt–$S^2$/$S^{2'}$, Pt–$S^1$/$S^{1'}$, Pt–$S^{2'}$/$S^2$, and Pt–$S^{1'}$/$S^1$ rearrangements the four isomers *cis*-1, *cis*-2, and the enantiomeric *trans* pair may be exchanged. However, *cis*-2 remained undetected and, furthermore, the band-shape fittings showed there to be negligible direct *trans* $\rightleftharpoons$ *trans** exchange. Thus the pivot process simply involves the exchanges *trans** $\underset{\text{rearrangement}}{\overset{\text{Pt–S}^{1'}\text{ S}^1}{\rightleftharpoons}}$ *cis*-1 $\underset{\text{rearrangement}}{\overset{\text{Pt–S}^{2'}\text{ S}^{2'}}{\rightleftharpoons}}$ *trans* and may be described as reciprocating clockwise/anticlockwise pivots about the ligand backbone C–C bond, arising from alternative Pt–$S^1$/$S^{1'}$ and Pt–$S^2$/$S^{2'}$ bond rearrangements.

Apart from representing the first example of metal pivoting in mononuclear platinum(IV) complexes, the process is novel in that the pivot occurs about a C–C bond rather than about a Pt–S bond as found previously in $[(PtXMe_3)_2L]$ complexes. Metal pivoting energy data for previously studied $[(PtBrMe_3)_2L]$ complexes are given in Table 7 and compared with data obtained from the present $[PtBrMe_3\{(MeS)_2CHCH(SMe)_2\}]$ complex and the related mononuclear complex $[PtBrMe_3(MeSCH_2SCH_2SMe)]$.[18] The $\Delta G^{\ddagger}$ values can be seen to decrease in the order $HC(SMe)_3 > \overline{S(CH_2)_4} > \overline{S(CH_2)_3}$. This suggests that the pivot is favoured when the non-co-ordinated S atom(s) is/are constrained by the ligand ring to more favourable positioning for achieving the pivot transition state. However, the ligand rotation angle is also clearly a controlling factor for the rate process. For instance, in the case of the $MeSCH_2SCH_2SMe$ complex,[18] the ligand undergoes 180° switches between the platinum pairs and clearly this large rotation angle is the main cause of the relatively high $\Delta G^{\ddagger}$ value. The exceptionally high $\Delta G^{\ddagger}$ value in the present complexes may be attributed to the relatively large pivot angle (109.5°) involved

*plus* the flexibility of the unco-ordinated, pendant S–methyl groups, both factors disfavouring easy access to the transition-state structure of the fluxional process.

## References


1 Part 1, E. W. Abel, T. P. J. Coston, K. M. Higgins, K. G. Orrell, V. Šik, and T. S. Cameron, preceding paper.
2 E. W. Abel, S. K. Bhargava, and K. G. Orrell, *Prog. Inorg. Chem.*, 1984, **32**, 1.
3 E. W. Abel, A. R. Khan, K. Kite, K. G. Orrell, and V. Šik, *J. Chem. Soc., Dalton Trans.*, 1980, 2208.
4 E. W. Abel, K. Kite, K. G. Orrell, V. Šik, and B. L. Williams, *J. Chem. Soc., Dalton Trans.*, 1981, 2439.
5 E. W. Abel, M. Booth, G. D. King, K. G. Orrell, G. M. Pring, and V. Šik, *J. Chem. Soc., Dalton Trans.*, 1981, 1846.
6 E. W. Abel, T. E. MacKenzie, K. G. Orrell, and V. Šik, *J. Chem. Soc., Dalton Trans.*, 1986, 2173.
7 E. W. Abel, M. Booth, K. G. Orrell, and G. M. Pring, *J. Chem. Soc., Dalton Trans.*, 1981, 1944.
8 E. W. Abel, T. E. MacKenzie, K. G. Orrell, and V. Šik, *Polyhedron*, 1987, **6**, 1785.
9 E. W. Abel, S. K. Bhargava, T. E. MacKenzie, P. K. Mittal, K. G. Orrell, and V. Šik, *J. Chem. Soc., Dalton Trans.*, 1987, 757.
10 E. W. Abel, K. M. Higgins, K. G. Orrell, V. Šik, E. H. Curzon, and O. W. Howarth, *J. Chem. Soc., Dalton Trans.*, 1985, 2195.
11 D. A. Kleier and G. Binsch, Program 165, Quantum Chemistry Program Exchange, Indiana University, 1970.
12 J. Jeener, B. H. Meier, P. Bachmann, and R. R. Ernst, *J. Chem. Phys.*, 1979, **71**, 4546.
13 S. Macura and R. R. Ernst, *Mol. Phys.*, 1980, **41**, 95.
14 C. L. Perrin and R. K. Gipe, *J. Am. Chem. Soc.*, 1984, **106**, 4036.
15 E. W. Abel, T. P. J. Coston, K. G. Orrell, V. Šik, and D. Stephenson, *J. Magn. Reson.*, 1986, **70**, 34.
16 J. H. Noggle and R. E. Schirmer, 'The Nuclear Overhauser Effect,' Academic Press, London and New York, 1971.
17 E. W. Abel, S. K. Bhargava, K. Kite, K. G. Orrell, V. Šik, and B. L. Williams, *J. Chem. Soc., Dalton Trans.*, 1982, 583.
18 E. W. Abel, M. Z. A. Chowdhury, K. G. Orrell, and V. Šik, *J. Organomet. Chem.*, 1983, **258**, 109.


*Received* 23*rd May* 1988; *Paper* 8/02031K